

Research Article: New Research | Cognition and Behavior

Spontaneous Fluctuations in Alpha Peak Frequency Along the Posterior-to-Anterior Cortical Plane

<https://doi.org/10.1523/ENEURO.0118-25.2025>

Received: 12 March 2025

Revised: 14 October 2025

Accepted: 21 October 2025

Copyright © 2025 Balaji et al.

This is an open-access article distributed under the terms of the [Creative Commons Attribution 4.0 International license](#), which permits unrestricted use, distribution and reproduction in any medium provided that the original work is properly attributed.

This Early Release article has been peer reviewed and accepted, but has not been through the composition and copyediting processes. The final version may differ slightly in style or formatting and will contain links to any extended data.

Alerts: Sign up at www.eneuro.org/alerts to receive customized email alerts when the fully formatted version of this article is published.

1. Manuscript Title (50 word maximum): Spontaneous Fluctuations in Alpha Peak Frequency Along the Posterior-to-Anterior Cortical Plane

2. Abbreviated Title (50 character maximum): Spontaneous Fluctuations in Alpha Peak Frequency

3. List all Author Names and Affiliations in order as they would appear in the published article:

Vaishali Balaji, Alfons Schnitzler, Joachim Lange

Institute of Clinical Neuroscience and Medical Psychology, Medical Faculty and University Hospital Düsseldorf, Heinrich Heine University Düsseldorf, Germany

4. Author Contributions: J.L. and A.S. designed research; V.B. and J.L. performed research and analysed data; V.B., A.S. and J.L. wrote the paper.

5. Correspondence should be addressed to (include email address): Vaishali Balaji at vaishali.balaji@med.uni-duesseldorf.de

6. Number of Figures: 4

9. Number of words for Abstract: 206

7. Number of Tables: 1

10. Number of words for Significance Statement: 120

8. Number of Multimedia: n/a

11. Number of words for Introduction: 720

12. Number of words for Discussion: 1368

1

13. Acknowledgements: This work was supported by the Deutsche Forschungsgemeinschaft. We also thank the MRI Core Facility at the Medical Faculty of University Hospital Düsseldorf for supporting the acquisition of MRIs.

14. Conflict of Interest: Authors report no conflict of interest

15. Funding sources: Deutsche Forschungsgemeinschaft (Project number 447849261)

2

3

4

5

6

7

8

9

10

11

12

Abstract

Alpha peak frequency (APF) is defined as a prominent spectral peak within the 8-12 Hz frequency range. Typically, an individual's alpha frequency is regarded as a stable

neurophysiological marker. A wealth of recent evidence, however, indicates that APF shifts within short timescales in relation to task demands and even spontaneously so. Further, brain stimulation studies often report shifts in APF both within and between experimental sessions, directly contradicting the idea of a stable APF. To characterise the non-stationarities in spectral parameters, we estimated APFs from one-second epochs of resting-state magnetoencephalography (MEG) recordings from healthy adults of either sex. To enhance signal-to-noise ratio, without compromising on temporal resolution, we averaged power spectra within parcelled regions. Our findings indicate that variation in APFs exacerbates along the posterior-to-anterior cortical plane i.e., from the occipital to the frontal cortices. Further, by comparisons with amplitude-matched simulated signals, we demonstrated that the observed gradient is not attributable to measurement noise. Across the cortex, APFs showed poor temporal reliability, raising the question of whether APFs are more like a transient state than a trait. In general, our study elucidates the dynamic characteristics of alpha oscillations and reveals systematic regional differences which are, in part, shaped by underlying signal-to-noise ratio inherent to MEG recordings.

Significance Statement

Oscillatory signals, as recorded with electro-/magneto- encephalography, exhibit a prominent peak in the Alpha frequency range (i.e., APF). It is widely accepted that the amplitude and phase of oscillatory signals vary with behaviour. However, the stability of APF within and across experimental sessions is seldom examined. In this study, we characterised the changes in APF to show that the degree of fluctuations in APF systematically increased from the occipital cortex to the frontal cortex, forming a gradient across the cortical surface. We also established that the observed variability was not driven by underlying noise. Our results raise the possibility that the dynamics of APF could be a salient feature of a cortical region, driven by its underlying structure and function.

1. Introduction

13 Alpha oscillations, within the 8-12 Hz frequency range, are a prominent feature of electro - and
14 magneto – encephalography (E/MEG) recordings (Berger, 1929). Parameters of the alpha
15 oscillations, such as power and phase, have been studied extensively in the context of neural
16 inhibition and excitation (Jensen et al., 2012; Jensen & Mazaheri, 2010; Klimesch et al., 2007;
17 Lange et al., 2013; VanRullen, 2016). Typically, these studies examined power and phase in
18 fixed or predefined frequencies or frequency bands. However, the practice of employing strict,
19 *a priori* defined, frequency bands might overlook potentially meaningful variation within the

20 alpha band (Donoghue et al., 2022; Jones et al., 2009; Sherman et al., 2016; Tallon-Baudry,
21 1999). Alpha peak frequency (APF), defined as the frequency having the maximum power, is
22 a distinct measure of oscillatory activity. As APF is estimated per individual from the empirical
23 data, it allows for flexible comparisons of intra- and inter- individual differences in behaviour
24 and cognition (Baumgarten et al., 2023).

25 Especially within the context of perception, APF has been widely implicated in the speed of
26 processing information. APF is said to determine the temporal resolution of the visual system
27 whereby fluctuations in APF dictate whether one perceives discrete visual stimuli as
28 simultaneous or separate (Drewes et al., 2022; Samaha & Postle, 2015; Sharp et al., 2022).
29 Similarly, top-down modulation of APF was demonstrated in the context of a working memory
30 paradigm with an increase in APF in conjunction with increased memory load (Babu Henry
31 Samuel et al., 2018; Haegens et al., 2014). Even in the absence of experimental manipulation,
32 Benwell et al., (2019) found a difference in APF between two halves of an experimental
33 session, whereas Cohen (2014) reported shifts in APFs within resting-state networks. Further,
34 Mahjoory and colleagues (2020) showed a systematic decrease of APF across the cortex in
35 the posterior to anterior direction, suggesting that APF varies spatially.

36 Contradictorily, it is assumed that APF is a stable 'trait' marker (Grandy et al., 2013; Haegens
37 et al., 2014). This view is mainly driven by the longitudinal changes in APF across the lifespan
38 in congruence with brain volume (Lindsley, 1939), and relative stability over test-retest intervals
39 (Kondacs & Szabó, 1999) despite cognitive interventions (Grandy et al., 2013). APF is
40 considered a neurophysiological fingerprint, especially due to its presumed heritability (Smit et
41 al., 2006) and marked inter-individual differences (Klimesch, 1999; Posthuma et al., 2001).
42 However, APF may resemble a state factor depending on the timescale of the investigation.
43 Conventional analyses, which estimate APF from 2-5 minutes of resting-state M/EEG, capture
44 the mean peak frequency over this time-period; however, the APF may spontaneously
45 fluctuate around the mean frequency in response to changes in physical stimuli or cognitive-
46 state. In fact, numerous non-invasive brain stimulation studies report the notoriety of matching
47 stimulation frequency to APF (Stecher & Herrmann, 2018; Vossen et al., 2015), highlighting
48 the practical pitfalls of assuming that APF remains stationary over time.

49 Findings from computational studies collectively suggest that frequency transitions within the
50 alpha band are likely a natural consequence of variation in synaptic input and concurrent firing
51 rates of neural populations (Hutt et al., 2016; Lefebvre et al., 2015). When firing rates increase
52 relative to baseline, cortical networks recruit non-linear feedback loops, in turn changing the
53 system's response function and the features of its emergent dynamics (Mierau et al., 2017).
54 Therefore, APF is a proxy for the activation-state of a population of neurons. As such, the

55 fluctuations of frequency are a dynamic signature of low-frequency neural oscillations, but they
56 are rarely accounted for in the analysis of experimental data.

57 Building on previous work by Smith et al., (2024), we aimed to analyse the stability of APF at
58 short timescales. To this end, we estimated individual APFs from source-reconstructed power
59 spectra derived from brief time-series (1s epochs) of resting-state magnetoencephalography
60 (MEG). We decomposed the power spectrum into periodic and aperiodic components,
61 ensuring that estimates of APF are unaffected by aperiodic activity. Since frequency of the
62 intrinsic oscillator may vary spontaneously in conjunction with synaptic input, we hypothesised
63 that APFs would show considerable variability within individuals. Further, brain areas vary in
64 terms of spectral profiles (Keitel & Gross, 2016; Mahjoory et al., 2020; Mellem et al., 2017),
65 developmental trajectories (Charvet & Finlay, 2014) and structural connections (Huntenburg
66 et al., 2017); hence, we hypothesised that the variability of APFs would also be spatially
67 heterogeneous.

2. Methods

2.1 Experimental design

68 In this study, we analysed a previously acquired dataset (manuscript has been submitted for
69 publication), containing around four minutes of resting- state MEG recordings from 24 healthy
70 participants (11 female, age 25.33 ± 2.81 [mean \pm SD] years). The participants were seated
71 upright in a dimly lit magnetically shielded room while we recorded neural activity using a 306-
72 channel MEG system, with a sampling frequency of 1000 Hz (MEGIN Oy, Finland).

73 The MEG recordings are from a study where transcranial alternating current stimulation (tACS)
74 was applied to the participants' somatosensory cortex. Each recording started with a baseline
75 period of 2 min, followed by periods of either 10s or 30s of tACS, or no stimulation (control).
76 The data used in the present study were collected during the control session. That is, tACS
77 electrodes were placed at the participants' scalp, but no electrical stimulation was
78 administered. The participants were unaware of the stimulation condition (10s, 30s, or control).
79 Hence, we classify this dataset as resting-state MEG.

80 In addition, we instructed participants to focus on a white fixation-cross through the duration of
81 the experiment. The cross was projected (PT-DW700E, Panasonic, Japan) on translucent
82 screen placed ~ 57 cm in front of the participants. The fixation-cross rotated by 45° for 500 ms
83 at random time points. Participants had to press a button within two seconds of the rotation.

84 This task served merely as a vigilance task paradigm and was included to ensure sustained
85 attention (Zaehle et al., 2010).

86 We acquired anatomical T1-weighted MRIs with a 3T Siemens scanner (Siemens Magnetom
87 Tim Trio 3T, Siemens, Germany). We used the Polhemus Fastrak system (Polhemus, USA) to
88 digitise HPI coils, fiducial markers, and ~50-100 additional points. We recorded
89 electrooculogram (EOG) to monitor blinks and eye movements.

2.2 MEG data preprocessing

90 Entire preprocessing and analysis of the datasets were performed using the Fieldtrip toolbox
91 (version 20240614) and custom-made scripts on MATLAB (R2023b; The MathWorks, Inc.,
92 USA).

93 We segmented the continuous MEG recording into trials, consisting of a single baseline trial
94 (110 s) and 20 resting-state trials (of ~5.5 s). We restricted further preprocessing to 204
95 gradiometer channels. We applied a band-pass filter of 4-150 Hz and removed the linear trends
96 and mean of every trial. We applied Fieldtrip's semi-automatic artefact detection approach to
97 remove segments of trials containing artefacts (e.g., SQUID jumps, head and muscle
98 movements). After visual inspection, we additionally removed noisy channels and trials
99 containing artefacts. We used Independent Component Analysis (ICA) to remove any
100 remaining electro-cardio and electro-ocular artefacts.

2.3 Source reconstruction

101 We reconstructed the sources of the time-series data measured by MEG sensors using
102 Linearly Constrained Minimum Variance (LCMV) beamformers (Van Veen et al., 1997).

103 We generated a single-shell volume conduction model by performing co-registration of the
104 sensors to participants' anatomical MRIs using fiducial markers, followed by segmentation of
105 the brain surface (Nolte, 2003). Then we divided the brain volume into a regular 3D-grid with
106 a 5 mm resolution, based on the MNI template brain (Montreal Neurological Institute, Canada).

107 We restricted the analysis to cortical regions resulting in 8384 grid points. We estimated spatial
108 filters for each of the cortical grid points along the dipole direction with maximal power, with a
109 regularisation parameter of 10%. By multiplying these filters with sensor-level data, we
110 reconstructed time-series data at the source. Subsequently, source-level time-series were
111 parcellated into 210 cortical regions of interest based on the Brainetome atlas (Fan et al.,
112 2016).

2.4 Data analysis

113 We concatenated baseline and resting-state trials to create a continuous segment of the time
114 series (~ 220 s) and then segmented parcel time-series into 1-s epochs. We computed power
115 spectra for each epoch using a multi-tapered (3 tapers) Fast Fourier transform, based on
116 discrete prolate spheroidal sequences (dpss), with 2 Hz spectral smoothing. We averaged
117 power spectra over grid points within each parcel, resulting in ~220 power spectra per parcel
118 and participant. We estimated the aperiodic 1/f component using the 'Fitting Oscillations One
119 Over F' (FOOOF; Donoghue et al., 2020) algorithm in Python 3.7.2. Then we subtracted the
120 1/f component from the corresponding spectra and determined the spectral peaks in the alpha
121 band (7-14 Hz), for each corrected spectrum of a parcel, using the 'findpeaks' function on
122 MATLAB. The frequency of the peak with the strongest power was regarded as the alpha peak
123 frequency (APF) of a given spectrum. Epochs without a definitive spectral peak i.e., a flat peak
124 with two neighbouring frequencies of the same power, were given the value of a 'NaN'.

2.5 Statistical analysis

125 First, we sought to replicate the results of Mahjoory et al., (2020). To this end, we performed a
126 linear regression between time-averaged APF of 210 parcels and their corresponding Y-
127 coordinate position, along the posterior-to-anterior direction. Second, to quantify the degree of
128 variation in APFs within participants, we calculated the Coefficient of Variation (CV), for a given
129 parcel, by dividing the standard deviation by the mean APF across 220 epochs. For a given
130 parcel, k :

$$CV_{parcel\ k} = \sigma_{epochs\ k} \div \mu_{epochs\ k}$$

131 To test the regional differences in CV along the posterior-anterior axis, we performed a linear
132 regression between CV values of all parcels and their corresponding Y-coordinate position.

133 To check whether the spatial profile of alpha power confounded the estimation of APF, we
134 calculated signal-to-noise ratio (SNR) and CV for each of the 8384 cortical grid points. We
135 defined SNR as the ratio between the power of the APF and the average power of spectral
136 peaks in all other frequencies. We averaged SNR and CV values within a spatial sliding window
137 of 2.5 cm in increments of 0.25 cm (along the posterior to anterior direction), resulting in 61
138 SNR and CV values per participant. We concatenated the CV and SNR values across
139 participants and performed a Pearson correlation.

140 To contrast the variation in APF with noise, we subjected 20 empty-room datasets to the same
141 preprocessing and data analysis steps as detailed in the foregoing sections. Additionally, we
142 added a 10 Hz alpha and a 20 Hz beta rhythm to the empty-room time series. The simulated
143 alpha peaks decreased in amplitude along the posterior to anterior direction, thereby mimicking
144 the physiological data (Fig. 3-1). The beta rhythm was added as a proxy to neuronal noise. We

145 obtained CV values for the 210 parcels of physiological data, CV values for 204 MEG sensor
146 channels of non-neuronal noise data and CV values for 204 MEG sensor channels of simulated
147 noise data. We averaged CV values along the Y-axis gradient using a spatially sliding window
148 as detailed above. Then we performed independent t-tests for each of the 61 Y-coordinate
149 positions between signal and noise data. To circumvent the multiple comparison problem, we
150 performed a non-parametric cluster-based permutation test. We permuted the data by shuffling
151 the condition assignment (signal vs noise). Spatially adjacent Y-coordinate positions, which
152 met *a priori* defined threshold ($\alpha = 0.05$), were combined to a cluster. On each permutation,
153 we retained the cluster with the maximum sum of t-values. Given 1000 summed cluster t-
154 values, obtained from 1000 permutations, we determined the probability of the empirical data.

155 To ensure that peaks identified from the physiological data reflected genuine neural activity
156 rather than ambient noise, we estimated the distribution of spectral peak powers across the
157 empty-room recordings (per MEG sensor), and we discarded epochs from physiological data,
158 if the identified APF did not exceed the 99th percentile of this noise distribution (see Fig. 3-2).
159 We then calculated CV values for all remaining APFs per parcel. To test whether the regional
160 differences in CV persisted after excluding APFs with low amplitudes, we performed a linear
161 regression between the recalculated CV values and their corresponding Y-coordinate position.

162 Finally, we examined whether APF is a stable “trait-like” construct which is distinguishable
163 between subjects. We used intra-class correlation (ICC) to measure the reliability of APF which
164 akin to intra-rater reliability, quantifies the variation of data measured by 1 rater across 2 or
165 more trials. In our study, it is the extent to which a single individual consistently produces the
166 same APFs across epochs. Specifically, we implemented a single-rater two-way mixed-effects
167 model and absolute agreement definition, or ICC(A,1) (McGraw & Wong, 1996; Shrout &
168 Fleiss, 1979). Generally, ICC is calculated as a ratio,

$$\frac{MS_B - MS_E}{MS_B + (k - 1)MS_E + \frac{k}{n}(MS_W - MS_E)}$$

169 where, MS_B is mean square between participants, representing the variance attributable to
170 true differences between individuals, MS_E is mean square for error, representing the residual
171 error variance (i.e., the variance not accounted for by participant or measurement), MS_W is the
172 mean square within participants, representing the variance between measurements, k is the
173 number of measurements (or epochs), and n is the number of participants. If the MS_E is equal
174 to or larger than the variance of interest (MS_B), the reliability of APFs is evidently poor.

175 ICC estimates and their 95% confidence intervals were calculated using the Matlab Central
176 file-exchange *ICC.m* function (Salarian, 2016). This ICC calculation was applied at every

177 parcel to obtain spatially specific reliability estimates. In addition, we estimated APFs from
178 epochs of 2 s and 5 s to chart out how ICC increases with longer periods of averaging (Fig. 4-
179 2 and 4-3). ICC estimates range from 0 – 1, with values closer to 1 indicating higher reliability.

3. Results

180 We successfully replicated the key results of Mahjoory et al., (2020) showing that APF
181 decreased significantly along the posterior-to-anterior axis ($R^2 = 0.646$, $p < 0.001$; Fig. 1-1).
182 The left lateral occipital cortex had the highest APF of 10.57 ± 1.61 Hz [mean \pm SD], whereas
183 the left middle frontal gyrus had the lowest APF of 7.5 ± 0.74 Hz [mean \pm SD].

184 To quantify changes in APF within participants, we calculated the CV for all cortical parcels.
185 CV values linearly increased along the posterior-to-anterior axis ($R^2 = 0.841$, $p < 0.001$; Fig.
186 1B). The lateral occipital cortices showed the least amount of variation in APF, with an average
187 CV of 0.13 ± 0.03 [mean \pm SD], whereas the superior and middle frontal gyri, showed the most
188 variation, with an average CV of 0.18 ± 0.01 . Among individuals, 70% showed a moderate
189 positive correlation between Y-coordinate position and CV ($r > 0.6$).

190 We found a significant negative correlation between SNR and CV ($r = -0.87$, $p < 0.001$; Fig. 2).
191 This suggests that low alpha power in the anterior regions may preclude the estimation of APF,
192 resulting in seemingly high CV. Alternatively, it could also be driven by the presence of multiple
193 alpha-band oscillations of comparable magnitude occurring simultaneously in anterior regions,
194 with APF switching between peaks as their relative prominence fluctuates.

195 To elucidate whether the temporal fluctuations in APF from second-to-second are simply a by-
196 product of noise, we contrasted APFs estimated from physiological data with APFs estimated
197 from empty-room measurements. CV of physiological signal was significantly lower than CV of
198 empty-room noise between -10.5 cm and 0 cm on the y-axis plane (i.e., from the occipital
199 cortex to pre-central gyri; Fig. 3A). In this significant spatial range, APF deviated by as much
200 as -2.2 to +1.7 Hz from the median in the physiological signal (Fig. 3B). To evaluate the integrity
201 of anterior APF estimates, we performed a control analysis in which we excluded epochs if the
202 identified APF did not exceed the threshold derived from empty-room recordings. We found a
203 substantial reduction in both the number of retained epochs and the CV values of the anteriorly
204 located parcels (Fig. 3-2). Such that only ~7% of epochs were retained in the frontal cortices,
205 whereas ~34% of epochs were retained in the occipital cortices. Notably, the linear increase
206 in CV values along the posterior-to-anterior axis was still evident ($R^2 = 0.359$, $p < 0.001$; Fig. 3-
207 2).

208 ICC estimates at each of the parcels showed the highest reliability in right precentral
209 (ICC = .121, 95% CI: .075-.216) and postcentral (ICC = .122, 95% CI: .075-.289) gyri, and
210 the left lateral occipital cortex (ICC = .123, 95% CI: .076-.219). The right superior frontal gyrus
211 (ICC = .018, 95% CI: .009-.040), and left middle frontal gyrus (ICC = .019, 95% CI: .010-.042;
212 Fig. 4) had the lowest reliability. Overall, ICC values across the cortex were indicative of poor
213 reliability of APF over epochs. The distribution of APFs in the left lateral occipital cortex of
214 individual participants (Fig. 4-1) indicate that low ICC values may reflect both limited
215 consistency within individuals and a lack of systematic differences between individuals.
216 Despite averaging power over longer segments of time (2 s and 5 s), even regions with the
217 highest ICC estimates (right lateral occipital cortex; ICC = 0.358, 95% CI: 0.244–0.531) fell
218 short of having adequate reliability (i.e., ICC > 0.5) (Fig. 4-2; Fig. 4-3). Consistently across all
219 epoch lengths, ICC estimates were highest in occipital regions and lowest in frontal regions.

4. Discussion

220 In recent years, alpha peak frequency (APF) has gained considerable attention as a potential
221 marker of human cognition. On the one hand, APF is highly heritable and resistant to change
222 over test-retest intervals, but on the other, it is extremely volatile and susceptible to changes
223 in task demands and shifts in intrinsic states (Mierau et al., 2017). In the present study, we
224 showed that such peak frequency transitions of APF occur at small timescales (i.e., within one
225 second) and the degree of variation in APF systematically increased from the caudal to rostral
226 regions. We established that the observed fluctuations and the spatial gradient were not just
227 an anomaly related to underlying noise. Further, we found that APFs show poor reliability
228 across time over the entire cortex.

229 First and foremost, we confirmed that APF decreases along the posterior-to-anterior axis in a
230 systematic fashion (in line with Mahjoory et al., 2020). The spatial gradient is governed by
231 differences in the geometry of the cortex, in terms of cytoarchitecture and connectivity
232 (Huntenburg et al., 2018), which in turn constrain the emergent dynamics (Demirtaş et al.,
233 2019; Shafiei et al., 2023). The temporal dynamics of APF, however, has been largely
234 overlooked. Therefore, we characterised the transient variations in APF to assess whether it
235 more closely resembles a state- than a trait-marker. Our results illustrate that, not only APF,
236 but also the degree of variation in APFs follows the posterior-to-anterior gradient, such that
237 fluctuations in APFs exacerbates along this direction. This is in line with the findings of Salinsky
238 et al., (1991) who provided evidence of variability on a similar timescale, but to a much smaller
239 degree. Recent findings reveal that the APF shows temporal variations on a sub-second scale,
240 evidently in the anterior regions (Smith et al., 2024), congruent with our findings. The temporal

241 features of regional signals are likely governed by the anatomical and functional connectivity
242 patterns with other cortical and subcortical regions. The caudal end of the gradient houses the
243 lower sensorimotor functions, whereas the rostral end oversees higher cognitive functions. In
244 effect, along the posterior-to-anterior direction, there is an increase in strength of synaptic
245 excitation (Wang, 2020) and density of neurotransmitter receptors (Luppi et al., 2022),
246 lengthening of timescales of information processing (Gao et al., 2020; Honey et al., 2012), and
247 weakening of the coupling between structure and function (Larivière et al., 2020). By virtue of
248 its neurobiological substrate, the rostral regions exhibit prolonged and flexible patterns of
249 activity which complements its function, requiring the synergistic integration of diverse inputs
250 (Suzuki et al., 2023). The results of our study are congruent in that respect. APF, reflecting
251 intrinsic neural timescales, is higher in the caudal pole, whereas variations in APF, indexing
252 input stochastics (Lefebvre et al., 2015) and neural malleability (Garrett et al., 2013), is higher
253 in the rostral pole.

254 We found the signal-to-noise ratio (SNR) systematically decreased along the posterior-to-
255 anterior axis, in relation to variations in APF. The alpha rhythm dominates the parieto-occipital
256 region, whereas beta (13-30 Hz) and theta (4-8 Hz) oscillations are prominent in the
257 sensorimotor and frontal regions, respectively (Groppe et al., 2013; Keitel & Gross, 2016). Due
258 to the variation in dominant peak frequency across the cortex, SNR varies on par. Given that
259 low power precludes the true estimation of APF, the variation in APFs along the posterior-to-
260 anterior axis may simply reflect an increment in noise/or a reduction in alpha power. However,
261 if that were to be the case, we would not expect to see a gradient in the parieto-occipital region.

262 We substantiated the variation in APFs along the gradient in comparison to noise, which was
263 recorded from an empty magnetically shielded room. These findings reaffirm that there is a
264 notable amount of variation in APFs from the occipital to the peri-central regions, following the
265 gradient, which is not seen in empty-room noise. On adding a 10 Hz rhythm to empty-room
266 noise, we found that the variation in empty room “APFs” was much lesser than APFs observed
267 in the physiological data, despite matching the amplitude of the simulated alpha and beta
268 rhythms. This leads us to believe that the variation in APFs did not arise from random
269 fluctuations in measurement noise. In the frontal regions, however, the amount of variation
270 was indistinguishable from non-neuronal noise, with the power of identified peaks being
271 comparable to the spurious peaks observed in the empty-room data. Therefore, we cannot
272 ascertain whether the degree of variation in the frontal regions is a manifestation of the intrinsic
273 neural dynamics. Due to the highly variable dynamics of the frontal regions, it is advisable to
274 exercise caution in conventional analyses, as estimates of alpha phase and coupling indices
275 may also be distorted by poor SNR (Aru et al., 2015; Donoghue et al., 2022).

276 Further, we found that estimates of reliability, as indexed by intra-class correlations (ICC), were
277 poor across the entire cortex in contrast to previous studies. A low ICC could be indicative of
278 low degree of agreement between measurements (i.e., substantial variability in APFs over
279 epochs) or a lack of difference in APFs between individuals (Koo & Li, 2016). Kondacs & Szabó
280 (1999) showed that APF has excellent reliability on comparing odd and even epochs of the
281 same EEG session. Another study found good reliability across two measurements, repeated
282 over the span of 10 months (Gasser et al., 1985). However, this study included a sample of
283 children, and as APFs and variability in neural signals changes over the course of development
284 (Mišić et al., 2010), it does not offer a direct comparison. In addition, these studies used scalp
285 recordings, which is inadequate to identify the sources of Alpha activity due to spatial mixing
286 of signals (Schaworonkow & Nikulin, 2022). Notably, in our dataset, averaging power spectra
287 over longer epochs drastically improved ICC estimates, but the observed values did not meet
288 the threshold for adequate reliability (Koo & Li, 2016). Therefore, our findings challenge the
289 reliability of APFs and suggest that it may not be a stable neurophysiological marker that
290 qualifies as a trait.

291 Our results challenge the common assumption that APF represents a stable, trait-like
292 characteristic—a premise that underlies many fixed-frequency stimulation protocols.
293 Stimulation paradigms targeting anterior alpha oscillations may be particularly vulnerable to
294 temporal variability, potentially failing to entrain neural oscillations. Furthermore, the dynamic
295 nature of alpha activity raises critical concerns for closed-loop stimulation approaches. If the
296 temporal resolution of such systems fails to capture the rapid shifts in endogenous oscillatory
297 parameters, stimulation may be mismatched with the targeted neural dynamics, thereby
298 compromising efficacy. In our study, participants were instructed to be seated such that the
299 back of their head is leaning against the fixed helmet of the MEG; therefore, the occipital cortex
300 lies closest to the SQUID sensor array, whereas the proximity of the frontal regions to the
301 sensor array varies between individuals. As a result, the magnitude of the signal, in relation to
302 background noise originating from non-neuronal sources, is much higher in the posterior
303 regions. However, the low reliability of APFs cannot simply be attributed to measurement
304 inaccuracies because despite good SNR, and a relatively low degree of variability in the
305 occipital region, the ICC estimates were not adequate (Boutros et al., 1991). Moreover, since
306 we only analysed datasets from a single measurement session, we cannot comment on the
307 trait-likeness of APF. Future studies would benefit from characterising the spatio-temporal
308 variations in APF over multiple sessions.

309 In general, the spectral parameters of alpha oscillations appear to be non-stationary over time.
310 Specifically, we showed that the degree of variation in APF increases along the posterior-to-
311 anterior direction. From the occipital to the pericentral regions, the variation in APFs was

312 evident in a substantial number of epochs, but still to a lesser extent than what is observed in
313 empty-room measurements, suggesting that the observed gradient is not a feature of
314 measurement noise. In the frontal regions, however, the degree of variation was
315 indistinguishable from noise, which highlights the necessity to consider temporal variability and
316 overall signal-to-noise ratio in the study of alpha oscillations. Further, the poor ICC estimates
317 obtained in our data suggest that, depending on the timescale of the investigation, APF could
318 transition rapidly, and to a similar extent across individuals, behaving more like a state than a
319 trait.

References

- Aru, J., Aru, J., Priesemann, V., Wibral, M., Lana, L., Pipa, G., Singer, W., & Vicente, R. (2015). Untangling cross-frequency coupling in neuroscience. *Current Opinion in Neurobiology*, 31, 51–61. <https://doi.org/10.1016/j.conb.2014.08.002>
- Babu Henry Samuel, I., Wang, C., Hu, Z., & Ding, M. (2018). The frequency of alpha oscillations: Task-dependent modulation and its functional significance. *NeuroImage*, 183, 897–906. <https://doi.org/10.1016/j.neuroimage.2018.08.063>
- Baumgarten, T. J., Wutz, A., & Samaha, J. (2023). Editorial: Peak frequencies in neural oscillatory activity and their connection to perception and cognition. *Frontiers in Psychology*, 14, 1234955. <https://doi.org/10.3389/fpsyg.2023.1234955>
- Benwell, C. S. Y., London, R. E., Tagliabue, C. F., Veniero, D., Gross, J., Keitel, C., & Thut, G. (2019). Frequency and power of human alpha oscillations drift systematically with time-on-task. *NeuroImage*, 192, 101–114. <https://doi.org/10.1016/j.neuroimage.2019.02.067>
- Berger, H. (1929). Über das elektroenkephalogramm des menschen. *Archiv Für Psychiatrie Und Nervenkrankheiten*, 87(1), 527–570.
- Boutros, N. N., Overall, J., & Zouridakis, G. (1991). Test-retest reliability of the P50 mid-latency auditory evoked response. *Psychiatry Research*, 39(2), 181–192. [https://doi.org/10.1016/0165-1781\(91\)90086-5](https://doi.org/10.1016/0165-1781(91)90086-5)

Charvet, C. J., & Finlay, B. L. (2014). Evo-Devo and the Primate Isocortex: The Central Organizing Role of Intrinsic Gradients of Neurogenesis. *Brain, Behavior and Evolution*, *84*(2), 81–92. <https://doi.org/10.1159/000365181>

Cohen, M. X. (2014). Fluctuations in Oscillation Frequency Control Spike Timing and Coordinate Neural Networks. *Journal of Neuroscience*, *34*(27), 8988–8998. <https://doi.org/10.1523/JNEUROSCI.0261-14.2014>

Demirtaş, M., Burt, J. B., Helmer, M., Ji, J. L., Adkinson, B. D., Glasser, M. F., Van Essen, D. C., Sotiropoulos, S. N., Anticevic, A., & Murray, J. D. (2019). Hierarchical Heterogeneity across Human Cortex Shapes Large-Scale Neural Dynamics. *Neuron*, *101*(6), 1181–1194.e13. <https://doi.org/10.1016/j.neuron.2019.01.017>

Donoghue, T., Haller, M., Peterson, E. J., Varma, P., Sebastian, P., Gao, R., Noto, T., Lara, A. H., Wallis, J. D., Knight, R. T., Shestyuk, A., & Voytek, B. (2020). Parameterizing neural power spectra into periodic and aperiodic components. *Nature Neuroscience*, *23*(12), 1655–1665. <https://doi.org/10.1038/s41593-020-00744-x>

Donoghue, T., Schaworonkow, N., & Voytek, B. (2022). Methodological considerations for studying neural oscillations. *European Journal of Neuroscience*, *55*(11–12), Article 11–12. <https://doi.org/10.1111/ejn.15361>

Drewes, J., Muschter, E., Zhu, W., & Melcher, D. (2022). Individual resting-state alpha peak frequency and within-trial changes in alpha peak frequency both predict visual dual-pulse segregation performance. *Cerebral Cortex*, *32*(23), 5455–5466. <https://doi.org/10.1093/cercor/bhac026>

Fan, L., Li, H., Zhuo, J., Zhang, Y., Wang, J., Chen, L., Yang, Z., Chu, C., Xie, S., Laird, A. R., Fox, P. T., Eickhoff, S. B., Yu, C., & Jiang, T. (2016). The Human Brainnetome Atlas: A New Brain Atlas Based on Connectional Architecture. *Cerebral Cortex*, *26*(8), 3508–3526. <https://doi.org/10.1093/cercor/bhw157>

Gao, R., Van Den Brink, R. L., Pfeffer, T., & Voytek, B. (2020). Neuronal timescales are functionally dynamic and shaped by cortical microarchitecture. *eLife*, *9*, e61277. <https://doi.org/10.7554/eLife.61277>

Garrett, D. D., Samanez-Larkin, G. R., MacDonald, S. W. S., Lindenberger, U., McIntosh, A. R., & Grady, C. L. (2013). Moment-to-moment brain signal variability: A

next frontier in human brain mapping? *Neuroscience & Biobehavioral Reviews*, 37(4), 610–624. <https://doi.org/10.1016/j.neubiorev.2013.02.015>

Gasser, T., Bächer, P., & Steinberg, H. (1985). Test-retest reliability of spectral parameters of the EEG. *Electroencephalography and Clinical Neurophysiology*, 60(4), 312–319. [https://doi.org/10.1016/0013-4694\(85\)90005-7](https://doi.org/10.1016/0013-4694(85)90005-7)

Grandy, T. H., Werkle-Bergner, M., Chicherio, C., Schmiedek, F., Lövdén, M., & Lindenberger, U. (2013). Peak individual alpha frequency qualifies as a stable neurophysiological trait marker in healthy younger and older adults. *Psychophysiology*, 50(6), Article 6. <https://doi.org/10.1111/psyp.12043>

Groppe, D. M., Bickel, S., Keller, C. J., Jain, S. K., Hwang, S. T., Harden, C., & Mehta, A. D. (2013). Dominant frequencies of resting human brain activity as measured by the electrocorticogram. *NeuroImage*, 79, 223–233. <https://doi.org/10.1016/j.neuroimage.2013.04.044>

Haegens, S., Cousijn, H., Wallis, G., Harrison, P. J., & Nobre, A. C. (2014). Inter- and intra-individual variability in alpha peak frequency. *NeuroImage*, 92, 46–55. <https://doi.org/10.1016/j.neuroimage.2014.01.049>

Honey, C. J., Thesen, T., Donner, T. H., Silbert, L. J., Carlson, C. E., Devinsky, O., Doyle, W. K., Rubin, N., Heeger, D. J., & Hasson, U. (2012). Slow Cortical Dynamics and the Accumulation of Information over Long Timescales. *Neuron*, 76(2), 423–434. <https://doi.org/10.1016/j.neuron.2012.08.011>

Huntenburg, J. M., Bazin, P.-L., Goulas, A., Tardif, C. L., Villringer, A., & Margulies, D. S. (2017). A Systematic Relationship Between Functional Connectivity and Intracortical Myelin in the Human Cerebral Cortex. *Cerebral Cortex*, 27(2), 981–997. <https://doi.org/10.1093/cercor/bhx030>

Huntenburg, J. M., Bazin, P.-L., & Margulies, D. S. (2018). Large-Scale Gradients in Human Cortical Organization. *Trends in Cognitive Sciences*, 22(1), 21–31. <https://doi.org/10.1016/j.tics.2017.11.002>

Hutt, A., Mierau, A., & Lefebvre, J. (2016). Dynamic Control of Synchronous Activity in Networks of Spiking Neurons. *PLOS ONE*, 11(9), e0161488. <https://doi.org/10.1371/journal.pone.0161488>

Jensen, O., Bonnefond, M., & VanRullen, R. (2012). An oscillatory mechanism for prioritizing salient unattended stimuli. *Trends in Cognitive Sciences*, 16(4), 200–206. <https://doi.org/10.1016/j.tics.2012.03.002>

Jensen, O., & Mazaheri, A. (2010). Shaping Functional Architecture by Oscillatory Alpha Activity: Gating by Inhibition. *Frontiers in Human Neuroscience*, 4. <https://doi.org/10.3389/fnhum.2010.00186>

Jones, S. R., Pritchett, D. L., Sikora, M. A., Stufflebeam, S. M., Hämäläinen, M., & Moore, C. I. (2009). Quantitative Analysis and Biophysically Realistic Neural Modeling of the MEG Mu Rhythm: Rhythmogenesis and Modulation of Sensory-Evoked Responses. *Journal of Neurophysiology*, 102(6), 3554–3572. <https://doi.org/10.1152/jn.00535.2009>

Keitel, A., & Gross, J. (2016). Individual Human Brain Areas Can Be Identified from Their Characteristic Spectral Activation Fingerprints. *PLOS Biology*, 14(6), e1002498. <https://doi.org/10.1371/journal.pbio.1002498>

Klimesch, W. (1999). EEG alpha and theta oscillations reflect cognitive and memory performance: A review and analysis. *Brain Research Reviews*, 29(2–3), 169–195. [https://doi.org/10.1016/S0165-0173\(98\)00056-3](https://doi.org/10.1016/S0165-0173(98)00056-3)

Klimesch, W., Sauseng, P., & Hanslmayr, S. (2007). EEG alpha oscillations: The inhibition–timing hypothesis. *Brain Research Reviews*, 53(1), Article 1. <https://doi.org/10.1016/j.brainresrev.2006.06.003>

Kondacs, A., & Szabó, M. (1999). Long-term intra-individual variability of the background EEG in normals. *Clinical Neurophysiology*, 110(10), 1708–1716. [https://doi.org/10.1016/S1388-2457\(99\)00122-4](https://doi.org/10.1016/S1388-2457(99)00122-4)

Koo, T. K., & Li, M. Y. (2016). A Guideline of Selecting and Reporting Intraclass Correlation Coefficients for Reliability Research. *Journal of Chiropractic Medicine*, 15(2), 155–163. <https://doi.org/10.1016/j.jcm.2016.02.012>

Lange, J., Oostenveld, R., & Fries, P. (2013). Reduced Occipital Alpha Power Indexes Enhanced Excitability Rather than Improved Visual Perception. *The Journal of Neuroscience*, 33(7), 3212–3220. <https://doi.org/10.1523/JNEUROSCI.3755-12.2013>

Larivière, S., Vos De Wael, R., Hong, S.-J., Paquola, C., Tavakol, S., Lowe, A. J., Schrader, D. V., & Bernhardt, B. C. (2020). Multiscale Structure–Function Gradients in the Neonatal Connectome. *Cerebral Cortex*, *30*(1), 47–58.

<https://doi.org/10.1093/cercor/bhz069>

Lefebvre, J., Hutt, A., Knebel, J.-F., Whittingstall, K., & Murray, M. M. (2015). Stimulus Statistics Shape Oscillations in Nonlinear Recurrent Neural Networks. *The Journal of Neuroscience*, *35*(7), 2895–2903.

<https://doi.org/10.1523/JNEUROSCI.3609-14.2015>

Lindsley, D. B. (1939). A Longitudinal Study of the Occipital Alpha Rhythm in Normal Children: Frequency and Amplitude Standards. *The Pedagogical Seminary and Journal of Genetic Psychology*, *55*(1), 197–213.

<https://doi.org/10.1080/08856559.1939.10533190>

Luppi, A. I., Mediano, P. A. M., Rosas, F. E., Holland, N., Fryer, T. D., O'Brien, J. T., Rowe, J. B., Menon, D. K., Bor, D., & Stamatakis, E. A. (2022). A synergistic core for human brain evolution and cognition. *Nature Neuroscience*, *25*(6), 771–782.

<https://doi.org/10.1038/s41593-022-01070-0>

Mahjoory, K., Schoffelen, J.-M., Keitel, A., & Gross, J. (2020). The frequency gradient of human resting-state brain oscillations follows cortical hierarchies. *eLife*, *9*, e53715.

<https://doi.org/10.7554/eLife.53715>

McGraw, K. O., & Wong, S. P. (1996). Forming inferences about some intraclass correlation coefficients. *Psychological Methods*, *1*(1), 30–46.

<https://doi.org/10.1037/1082-989X.1.1.30>

Mellem, M. S., Wohltjen, S., Gotts, S. J., Ghuman, A. S., & Martin, A. (2017). Intrinsic frequency biases and profiles across human cortex. *Journal of Neurophysiology*, *118*(5), 2853–2864. <https://doi.org/10.1152/jn.00061.2017>

Mierau, A., Klimesch, W., & Lefebvre, J. (2017). State-dependent alpha peak frequency shifts: Experimental evidence, potential mechanisms and functional implications. *Neuroscience*, *360*, 146–154.

<https://doi.org/10.1016/j.neuroscience.2017.07.037>

Mišić, B., Mills, T., Taylor, M. J., & McIntosh, A. R. (2010). Brain Noise Is Task Dependent and Region Specific. *Journal of Neurophysiology*, *104*(5), 2667–2676. <https://doi.org/10.1152/jn.00648.2010>

Nolte, G. (2003). The magnetic lead field theorem in the quasi-static approximation and its use for magnetoencephalography forward calculation in realistic volume conductors. *Physics in Medicine and Biology*, *48*(22), Article 22. <https://doi.org/10.1088/0031-9155/48/22/002>

Posthuma, D., Neale, M. C., Boomsma, D. I., & De Geus, E. J. C. (2001). [No title found]. *Behavior Genetics*, *31*(6), 567–579. <https://doi.org/10.1023/A:1013345411774>

Salarian, A. (2016). „MATLAB Central File Exchange. Intraclass Correlation Coefficient (ICC),”.

Salinsky, M. C., Oken, B. S., & Morehead, L. (1991). Test-retest reliability in EEG frequency analysis. *Electroencephalography and Clinical Neurophysiology*, *79*(5), 382–392. [https://doi.org/10.1016/0013-4694\(91\)90203-G](https://doi.org/10.1016/0013-4694(91)90203-G)

Samaha, J., & Postle, B. R. (2015). The Speed of Alpha-Band Oscillations Predicts the Temporal Resolution of Visual Perception. *Current Biology*, *25*(22), Article 22. <https://doi.org/10.1016/j.cub.2015.10.007>

Schaworonkow, N., & Nikulin, V. V. (2022). Is sensor space analysis good enough? Spatial patterns as a tool for assessing spatial mixing of EEG/MEG rhythms. *NeuroImage*, *253*, 119093. <https://doi.org/10.1016/j.neuroimage.2022.119093>

Shafiei, G., Fulcher, B. D., Voytek, B., Satterthwaite, T. D., Baillet, S., & Misic, B. (2023). Neurophysiological signatures of cortical micro-architecture. *Nature Communications*, *14*(1), 6000. <https://doi.org/10.1038/s41467-023-41689-6>

Sharp, P., Gutteling, T., Melcher, D., & Hickey, C. (2022). Spatial attention tunes temporal processing in early visual cortex by speeding and slowing alpha oscillations. *The Journal of Neuroscience*, JN-RM-0509-22. <https://doi.org/10.1523/JNEUROSCI.0509-22.2022>

Sherman, M. A., Lee, S., Law, R., Haegens, S., Thorn, C. A., Hämäläinen, M. S., Moore, C. I., & Jones, S. R. (2016). Neural mechanisms of transient neocortical beta rhythms: Converging evidence from humans, computational modeling, monkeys, and mice. *Proceedings of the National Academy of Sciences*, 113(33).

<https://doi.org/10.1073/pnas.1604135113>

Shrout, P. E., & Fleiss, J. L. (1979). Intraclass correlations: Uses in assessing rater reliability. *Psychological Bulletin*, 86(2), 420–428. <https://doi.org/10.1037/0033-2909.86.2.420>

Smit, C. M., Wright, M. J., Hansell, N. K., Geffen, G. M., & Martin, N. G. (2006). Genetic variation of individual alpha frequency (IAF) and alpha power in a large adolescent twin sample. *International Journal of Psychophysiology*, 61(2), 235–243.

<https://doi.org/10.1016/j.ijpsycho.2005.10.004>

Smith, M. K., Grabowekcy, M., & Suzuki, S. (2024). *Dynamic formation of a posterior-to-anterior peak-alpha-frequency gradient driven by two distinct processes.*

<https://doi.org/10.1101/2024.01.31.578276>

Stecher, H. I., & Herrmann, C. S. (2018). Absence of Alpha-tACS Aftereffects in Darkness Reveals Importance of Taking Derivations of Stimulation Frequency and Individual Alpha Variability Into Account. *Frontiers in Psychology*, 9, 984.

<https://doi.org/10.3389/fpsyg.2018.00984>

Suzuki, S., Grabowekcy, M., & Menciloglu, M. (2023). *Characteristics of spontaneous anterior-posterior oscillation-frequency convergences in the alpha band.*

<https://doi.org/10.1101/2023.09.12.557455>

Tallon-Baudry, C. (1999). Oscillatory gamma activity in humans and its role in object representation. *Trends in Cognitive Sciences*, 3(4), 151–162.

[https://doi.org/10.1016/S1364-6613\(99\)01299-1](https://doi.org/10.1016/S1364-6613(99)01299-1)

Van Veen, B. D., Van Drongelen, W., Yuchtman, M., & Suzuki, A. (1997). Localization of brain electrical activity via linearly constrained minimum variance spatial filtering. *IEEE Transactions on Biomedical Engineering*, 44(9), Article 9.

<https://doi.org/10.1109/10.623056>

VanRullen, R. (2016). Perceptual Cycles. *Trends in Cognitive Sciences*, 20(10), 723–735. <https://doi.org/10.1016/j.tics.2016.07.006>

Vossen, A., Gross, J., & Thut, G. (2015). Alpha Power Increase After Transcranial Alternating Current Stimulation at Alpha Frequency (α -tACS) Reflects Plastic Changes Rather Than Entrainment. *Brain Stimulation*, 8(3), Article 3. <https://doi.org/10.1016/j.brs.2014.12.004>

Wang, X.-J. (2020). Macroscopic gradients of synaptic excitation and inhibition in the neocortex. *Nature Reviews Neuroscience*, 21(3), 169–178.

Zaehle, T., Rach, S., & Herrmann, C. S. (2010). Transcranial Alternating Current Stimulation Enhances Individual Alpha Activity in Human EEG. *PLoS ONE*, 5(11), Article 11. <https://doi.org/10.1371/journal.pone.0013766>

Figure 1: Variation in alpha peak frequency

A) Exemplary demonstration of shifts in alpha peak frequency (APF) in three consecutive epochs. The left panel shows shifts in APF in the left lateral Occipital cortex from 9 Hz to 10 Hz, and then back to 9 Hz, all within three seconds. The right panel shows shifts in APF in the right superior Parietal Lobule from 9 Hz to 11 Hz, and then to 10 Hz, again within three seconds. **B)** In the left panel, the degree of variation in APF, measured by Coefficient of Variation (CV), is projected on an MNI template brain. In the right panel, CV values were averaged along a spatially sliding window in the posterior-to-anterior direction. Y-coordinate position of the parcel significantly predicted CV ($R^2 = 0.841$, $p < 0.001$). APF itself decreased significantly along the posterior-to-anterior axis (Fig. 1-1).

320

Figure 2: Correlation between CV and Signal-to-Noise ratio (SNR)

SNR of a parcel spectrum is the relative difference between the power of the APF and the average power of all other peak frequencies. The colour bar indicates the Y-coordinate position of each data point. Lighter colours lie caudally, whereas darker shades lie rostrally along the Y-coordinate axis. We found a significant negative correlation between SNR and CV, such that a lower SNR was associated with a higher degree of variation (CV) in APF ($r = -0.87$, $p < 0.001$).

Figure 3: Analysis of CV in relation to simulated signal and noise

A) The CV of physiological signal (in teal), non-neuronal noise (in grey) and simulated noise+signal (in blue) is plotted along the Y-coordinate plane. The shaded region indicates the standard deviation across datasets. On comparing physiological signal with empty-room noise, we found a statistically significant cluster between -10.5 cm and 0 cm (i.e., from the occipital cortex to the pre-central gyri). On contrasting physiological signal with simulated noise (i.e., Noise + 10 Hz + 20Hz), we found a statistically significant cluster across the entire cortex. Simulated alpha and beta peaks show amplitudes comparable to the physiological data (Fig. 3-1). The linear increase in CV values along the posterior-to-anterior axis remains evident after excluding APFs that did not meet the threshold (Fig. 3-2). **B)** Probability density of APF,

illustrating the distribution of APF shifts from the median APF of a parcel within the significant spatial cluster (between -10.5 cm and 0 cm).

Figure 4: Estimates of Intra-Class Correlation (ICC)

ICC values of each parcel are projected on an MNI template brain. Lower estimates of ICC indicate poor reliability, whereas higher estimates are indicative of better reliability. Overall, APF shows poor reliability across the cortex reflecting substantial shifts in APF throughout. Distribution of APFs in the left lateral occipital cortex across participants (Fig. 4-1), show that low ICC values may reflect limited consistency within individuals and a lack of systematic differences between individuals. ICC estimates for 2-s (Fig. 4-2) and 5-s (Fig. 4-3) epochs reveal highest reliability in occipital regions and lowest in frontal regions.

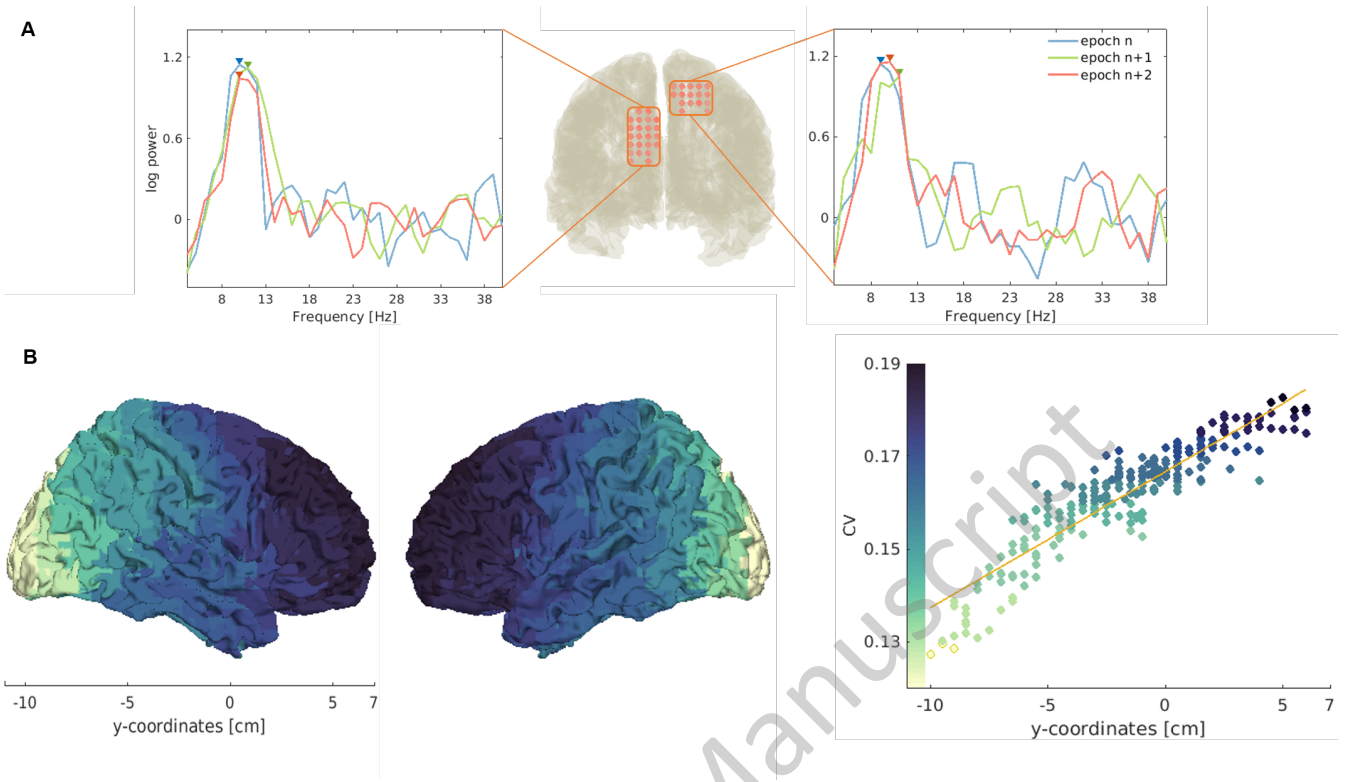
Table 1. Results of statistical tests

Figure	Comparison	Type of test	Statistic	95 % CI
1B	CV and y-coordinate of parcel	Linear regression	$R^2 = 0.841$, $p < 0.001$	[0.807, 0.871]
2	CV and SNR	Pearson correlation	$r = -0.87$, $p < 0.001$	[-0.878, -0.861]
3A	CV of signal and noise	Cluster-based permutation	Cluster statistic = -241.39, $p < 0.001$	CI range: [.002]
4	APFs of parcels	Intra-class correlation (ICC)	right precentral: ICC = .121 right superior frontal gyrus: ICC = .018	[0.075, 0.216] [0.009, 0.040]

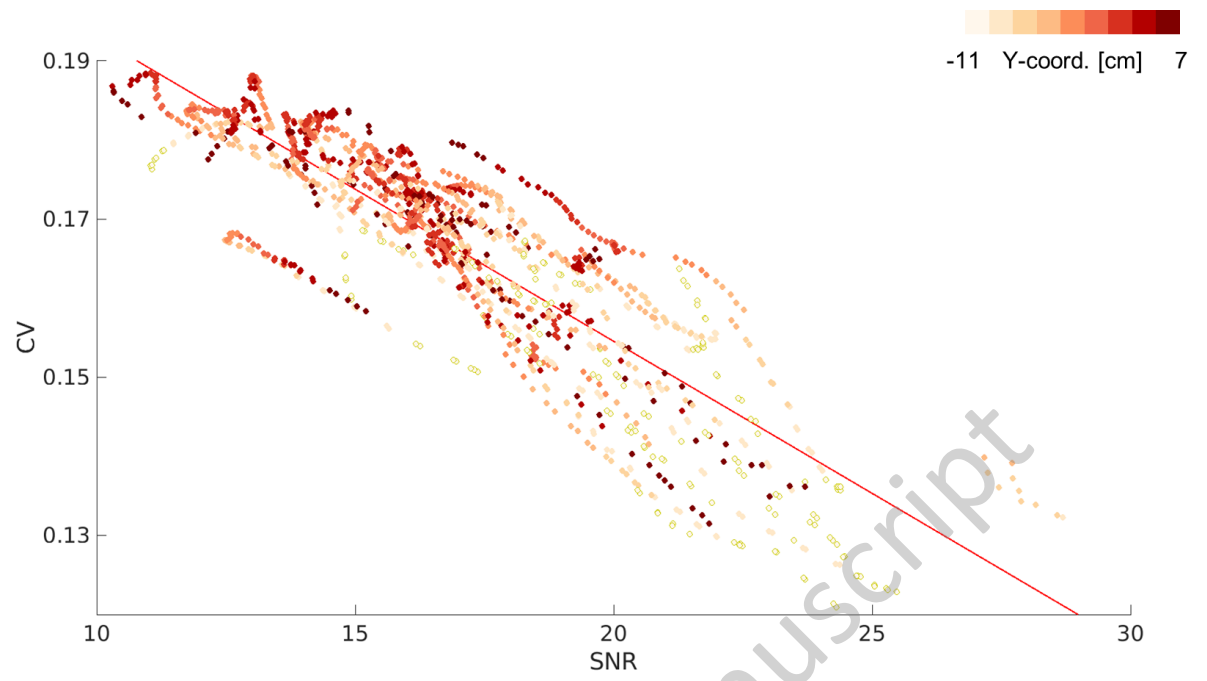
322

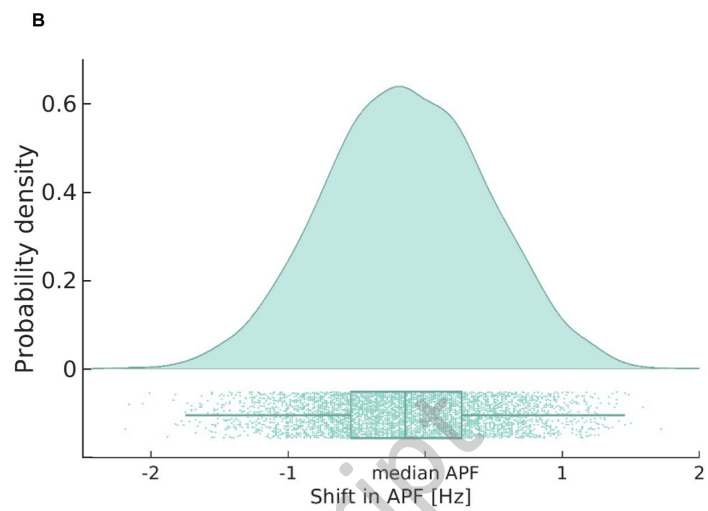
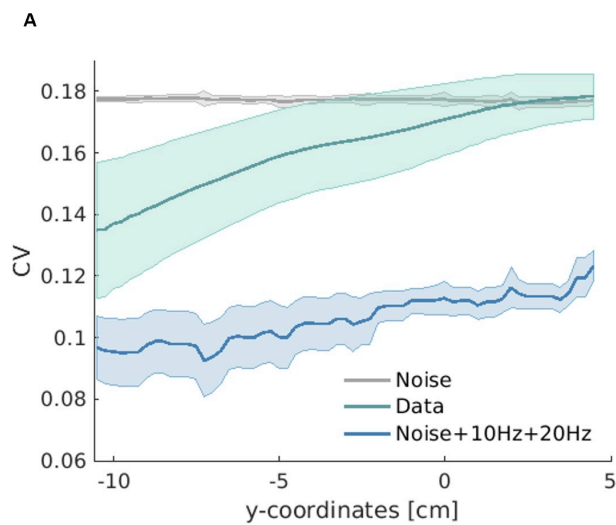
323

eNeuro Accepted Manuscript

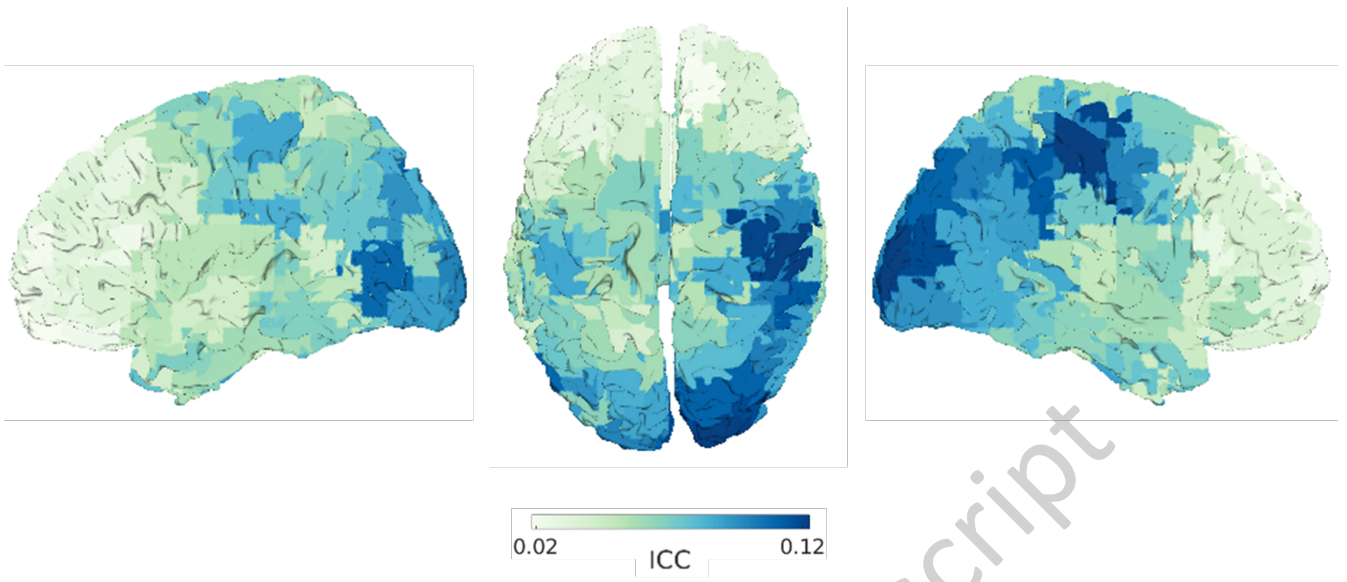


eNeuro Accepted Manuscript





eNeuro Accepted Manuscript



eNeuro Accepted Manuscript